한국윤활학회지(1995), 제 11 권 제 5 호
Journal of KSTLE(1995) Vol. 11, No. 5, pp.114~121

Non-Destructive Detection of Hertzian Contact Damage in Ceramics

H.S. Ahn* and S. Jahanmir**

**Korea Institute of Science and Technology, Seoul, Korea*
***National Institute of Standards and Technology, Gaithersburg, Maryland, U.S.A.*

Aestract—An ultrasonic technique using normal-incident compressional waves was used to evaluate the surface and subsurface damage in ceramics produced by Hertzian indentation. Damage was produced by a blunt indenter (tungsten carbide ball) in glass-ceramic, green glass and silicon nitride. The damage was classified into two types; (1) Hertzian cone crack, in green glass and fine grain silicon nitride, and (2) distributed subsurface micro fractures, without surface damage, produced in glass ceramic. The ultrasonic technique was successful in detecting cone craks. The measurement results with the Hertzian cone cracks indicated that cracks perpendicular to the surface could be detected by the normal-incident compressional waws. Also shown is the capability of normal-incident compressional waves in detection distributed micro-sized cracks size of subsurface microfractures.

Key words : Ultrosonic detection, Damage, Subsurface microfracture, Cone crack, Ceramics

1. Introduction

Surface of ceramic components in service are commonly subjected to concentrated loads. The contact stresses can introduce localized structural damage, which in turn can degrade the strength (Lawn and Marshall, 1978). Localized damage can also be ceramics. Surface and subsurface damage induced by machining are yet to be avoidable and these play a vital role on the mechanical performane of these materials (Jahanmir, 1993). The damage that occurs in the ceramics under Hertzian loading varies from Hertzian cone cracks to subsurface microfractures depending on the microstructural scale. In the present study, we use the spherical indenter configuration of Fig. 1; the indentation is said to be blunt. In its initial stages of loading the stress field is purely elastic, i.e. the classical Hertzian stress field applies. Beyond a critical load the material undergoes irrevesile deformation and/or fracture. In highly brittle materials such as glasses, single crystals, and ultrafine-grain polycrystals a ring crack initiates in the weakly tensile region just outside the circle of contact within the indenting sphere, propagates downward and outward into the material as a surface-truncated cone; i.e. a well-defined cone-shaped crack, the Hertzian fracture (Lawn, 1968; Lawn and Marshall, 1978). Recently, examination of Hertzian indentations in a coarse-grain polycrystalline alumina (Guiberteau *et al.*, 1994), coarse-grain silicon nitride (Xu *et al.*, 1995) and glass-ceramics (Cai *et al.*, 1994) have revealed a radical departure from the classical fracture pattern: the cone crack is suppressed in favor of distributed damage in a zone of high compression-shear below the contact circle. The subsurface damage takes the form of deformation/microfracture by precursor intragrain twin/slip and subsequent grain-localized intergranular micrfracture. It was shown that the transition from cone crack to accumulated microfracture zone occurs above a threshold grain size, indicating a microstructural scaling effect (Guiberteau *et al.*, 1994).

The purpose of this paper is to evaluate the ultrasonic method for the detection of surface and subsurface damage in ceramics induced by Hertzian contact.Although substantial effort has been devoted to the development and evaluation of NDE (Nondestructive evaluation) techniques for advanced ceramics, it was not until the early 80's that several NDE techniques such as ultrasonic detection, thermal wave imaging and micro-radiography became accessible to the detection of micro-sized suburface damage (Rocenswaing *et al.*, 1985; Edwards, 1988; Friedman *et al.*, 1988). In particular, ultrasound re-

lated techniques have been proved to be highly effective for assessing surface and near-surface damage in ceramics and are promising in view of their superiority other techniques for practical use as an in-process monitoring. Several publications have addressed the application of leaky surface wave(i.e., wave propagation parallel to the surface) for the detection of subsurface damage through acoustic microscopy (Yamanaka and Enomoto, 1982; Yamanaka *et al.*, 1985; Lawrence *et al*, 1990; Ahn and Achenbach, 1991). The acoustic microscopy offers an ability to image the subsurface features in materials which are opaque to other types of radiation. With high frequency transducers, detection of small surface and subsurface flaws undetectable by conventional ultrasonic methods is possible by acoustic microscopy.

In contrast with the leaky surface waves, the normal-incident compressional wave is advantageous over the acoustic microscopy for in-line application at manufacturing sites as it is less costly. An evaluation of the normal-incident compressional wave made recently for the detection of surface and subsurface damage in ceramics produced by a sharp indenter (Ahn *et al.*, 1994). The normal incident compressional wave technique in the study was successfully applied to detect lateral cracks while difficulty is experienced to discern the vertical cracks. Focusing of the transducer into the material (defocusing) provided information on the subsurface damage of materials. Furthermore the normal incident ultrasound techniques have demonstrated the accessibility to subsurface damage.

In this paper, well-defined Hertzian cone crack and accumulated subsurface microfractures generated by WC spherical indenter in green, glass-ceramic and silicon nitride are evaluated by the ultrasonic method using normal-incident compressional waves. The crack system produced by indentation in these materials probably represents a severe form of damage that may be present in machined surfaces. Therefore, analysis of these cracks provides a measure for the sensitivity of the ultrasonic method using mormal-incident compressional waves.

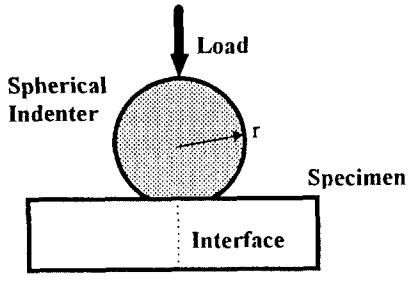

Fig. 1. Hertzian loading geometry for bonded-interface specimen.

2. Specimen Preparation

Three types of materials, silicon nitride, mica-containing glass-ceramic and green glass, were selected for this study. A hot-isostatically pressed silicon nitride (NBD200) with a grain size less than 1 μm was selected to represent a high strength ceramic while a mica-containing glass-ceramic was selected to represent a machinable ceramic. Silicon nitrides are attractive due to their high strength at elevated temperatures, resistance to chemical degradation, wear resistance and low density. Glass-ceramics are known for their easy machinability, an attractive quality for forming operations used in dental restorations (Chyung, 1974). The green glass was used as a reference material from which the mica-containing glass-ceramic is derived. As the damage type relies on the grain size, cone cracks were produced in a fine grain silicon nitride and a glass while subsurface microfractures were produced in a mica-containing glass-ceramic. The specimens were polished to reduce the influence of surface roughness on the measurements. The mica-containing glass-ceramic specimen was supplied by Cai et al. that was used in their analysis of fracture behavior (Cai *et al.*, 1994). For detailed microscopic investigation of the subsurface damage, they employed a special bonded-interface specimen, as shown in Fig. 1, which was fist used by Mulhearn (Mulhearn, 1959). All the indentaions except green glass were made using a tungsten carbide sphere of radius r=3.18 mm. The indentation in glass was made using a tungsten carbide sphere of radius r=4.76 mm. The indentation loads applied were 500 N, 1000 N and 1500 N for the mica-containing glass-ceramic, 400 N for green glass, and 4750 N for fine grain silicon nitride. Fig. 2 shows the optical microraphs of the indent in green glass. The bottom micrograph showing the cross-section view of the indent was obtained from a bonded-interface specimen (Cai *et al.*, 1994). The cone-shap-

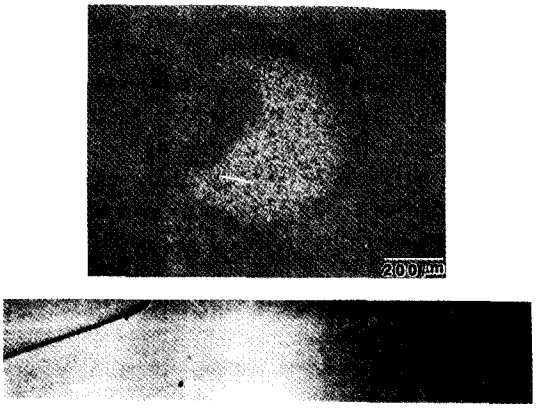

Fig. 2. Optical micrographs of indented green glass, showing surface (top) and section (bottom) views of Hertzian cone crack.

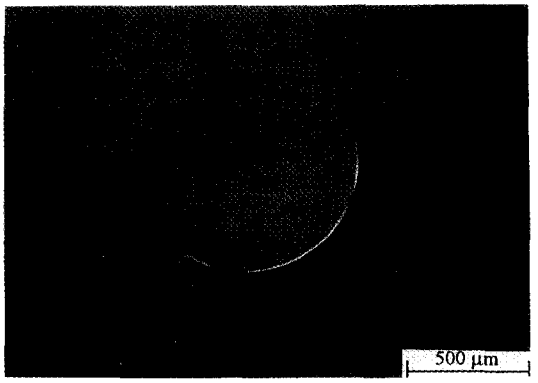

Fig. 3. Optical micrograph of indented silicon nitride, showing ring-shape crack just outside of the contact circle.

ed crack geometry is well developed. The contact radius lies within the ring, confirming that the cone crack forms in the region of weak tension outside the subsurface compression-shear zone Fig. 3 is the optical micrograph of the indent in fine silicon nitride. There is a conspicuous opening of the ring crack in lower region but in the rest the crack is closed.

Micrographs of analogous half-surface and side view of the mica-containing glass-ceramic were shown in Fig. 4 that are supplied from Cai et al. It is shown that cone crack outside the contact area is inactive. In Fig. 4(a), an accumulated microfractures damage starts subsurface and in Fig. 4(b), the damage is more developed, progressing toward the surface under a higher load, and in Fig. 4(c), eventually reaches the surface at the highest load, form-

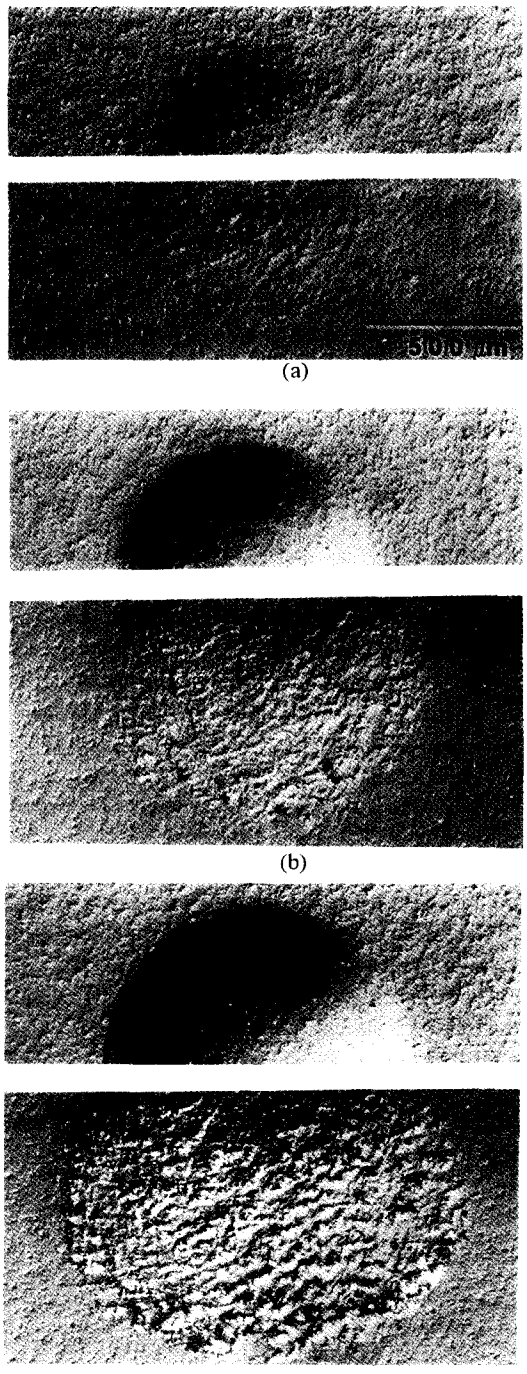

Fig. 4. Optical micrographs of indented glass-ceramic, showing half-surface (top) and section (bottom) views of subsurface microfracture damage in bonded-interface specimens, at indentation load (a) 500 N, (b) 1000 N and (c) 1500 N. (By the permission of Cai *et al.*)

ing a full plastic zone. It must be noted that there is an appearance of an intact near-surface region immediately below the surface, even under the highest load impression.

3. Ultrasonic Measurements

In ultrasonic measurement, normal-incident compressional pulsed waves generated by noncontact transducers are applied to determine surface and near-surface material characteristics, and to distinguish them from surface topographical features based on the measure of intensity of the echo signals from the examined specimen. At least two mechanisms pertain wheren the echo amplitude of this wave type may be affected by surface and subsurface damage: (i) an increased material compliance especially due to shallow horizontal subsurface cracks, and (ii) phase interference between surface reflections and subsurface reflections from within the material penetration depth.

3-1. Measurement System

The ultrasonic system, schematically illustrated in Fig. 5, consists of a broadband pulser/receiver, a gate detector, an oscilloscope, a digital voltmeter, a personal computer, and a computer-controlled 4-axis scanning stage (X, Y, Z, and ϕ) for line and raster scan. The specimens were immersed in a water bath coupling medium through which the pulsed wave travelled to and back from the specimen. The transducer was attached to a 4-axis scanning stage and used to tansmit and receive ultrasonic signals in conjunction with a pulser/receiver unit The measurements were carried out using a sharp-focused 50 MHz transducer with a spherical lens (focal length of 5.9 mm and fnumber of 0.8) to generate short wave pulses less than 0.1 μs in duration. This transducer produced a measured half-amplitude beam width (known as the effective beam width) of 30 to 35 μm in water at laboratory temperature. The actual operating frequency of this transducer was measured to be 35 MHz. At this operating frequency, the ultrasonic wave length in water is 43 μm. The gated peak detector acquires peak amplitude values in voltage from the reflected ultrasonic signals when selected area of specimen is scanned. The peak amplitude data were then read and recorded by the personal computer through an analog to digital converter board. The step size of the raster scan was 5 μm in both x and y direction.

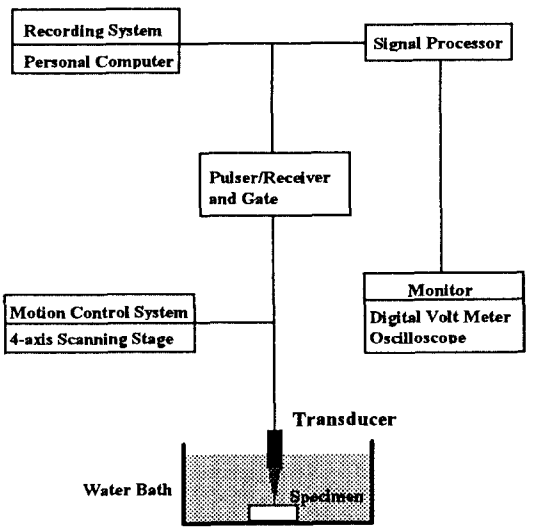

Fig. 5. Schematic diagram of the ultrasonic measurement system.

3-2. Detection of Hertzian Contact Damage

The result of ultrasound raster scan for the indent in glass, using normal-incident waves, is shown in Fig. 6(a) as an echo-amplitude 3-D map. The annular echo amplitude peak, which is resulted by a high reflection characteristics of sharp crack edges, defines the immediate inner region of the ring crack. in Fig. 6(b), a line scan along the center of the indent shows the precise location of ring crack, presented as the region of minimum echo-amplitude indicated by arrows. The distance between the two minimum is around 740 μm which is in good agreement with the diameter of the ring crack in the micrograph in Fig. 2

The result for ultrasonic examination of the indent in fine grain silicon nitride is shown in Fig. 7 By contrast to the result for the indent in green glass, there appears no echo-amplitude peak. In the region of open crack, more conspicnous reduction in the echo-amplitude is observed. Note that the normal incident compressional waves used in this study is unable to pinpoint the closed crack as it responds like an undamaged material.

Figure. 8 shows the result of the ultrasonic measurement on the indents in glass-ceramic. The 3-D echo-amplitude map in Fig. 8(a), and the contour

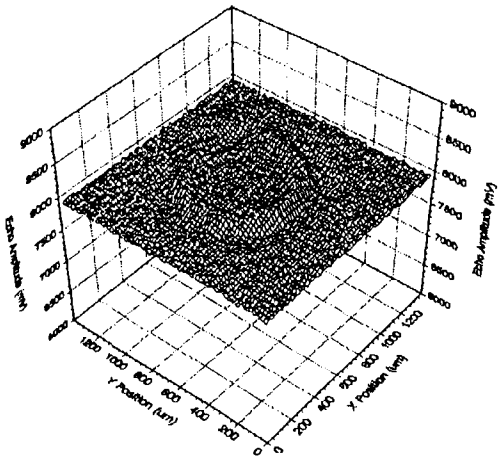

(a)

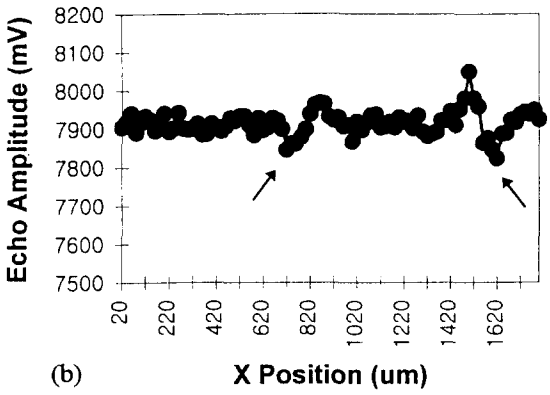

(b)

Fig. 6. 3-D echo-amplitude map of the indent in green glass, (a) and line scan over the center of the indent, (b).

map in Fig. 8(b), for the large indent show a reduction in the echo-amplitude corresponding to the periphery of the indent. This is resulted by the indent geometry. On the other hand, there is an increase in echo-amplitude inside the indent cirle. Careful examination of the indented surface revealed that the surface became smoother after indentation and thereby the reflectivity at surface was increased which in turn caused the higher amplitude of the returning echo. It can be noted that as the subsurface microfractures are sufficiently deep the ultrasonic measurement by focusing on the surface is unable to feature the subsurface damage. In an attempt to increase the sensitivity of ultrasonic pulses to subsurface microfractures, the transducer was focused below the surface. This is often referred to as detection of lateral cracks located below surface produced by Vickers indentation (Ahn *et al.*, 1994).

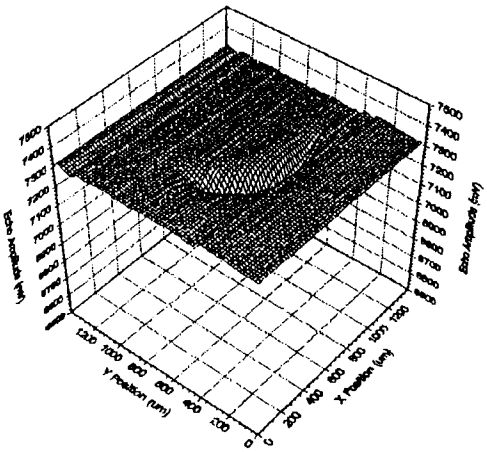

Fig. 7. 3-D echo-amplitude map of the indent in fine grain silicon nitride.

Fig. 8(b) shows the 3-D echo-amplitude map obtained at a focusing depth of 100 μm below surface. It is shown that the distributed microfractures below the surface is detected by defocusing the transducer, resulting in the substancial drop in the echo-amplitude. Therefore the detection capability of subsurface damage by normal-incident compressional waves is clearly demonstrated. This is further confirmed in the followings.

Fig. 9(b) shows the line scans at various depths of focus, z, which are passing over the indent center, as shown in figure (a). When the transducer is focused at the surface, the topographical influence of the indent is again observed regardless of the size of the indent, as the decrease and increase in the echo-amplitude in the periphery of the indent and inside indent circle, respectively. The line scan results at various depths of defocusing, show conspicuous drop in the echo-amplitude at the region below the indent surface. It must be noted that when the defocusing depth increases the influence of damage zone on the intensity of reflected ultrasonic pulses increases as the ultrasonic waves travel more into and back from the damage zone.

4. Discussion

In the present study, we utilized an normal-incident compressional ultrasonic waves to analyze

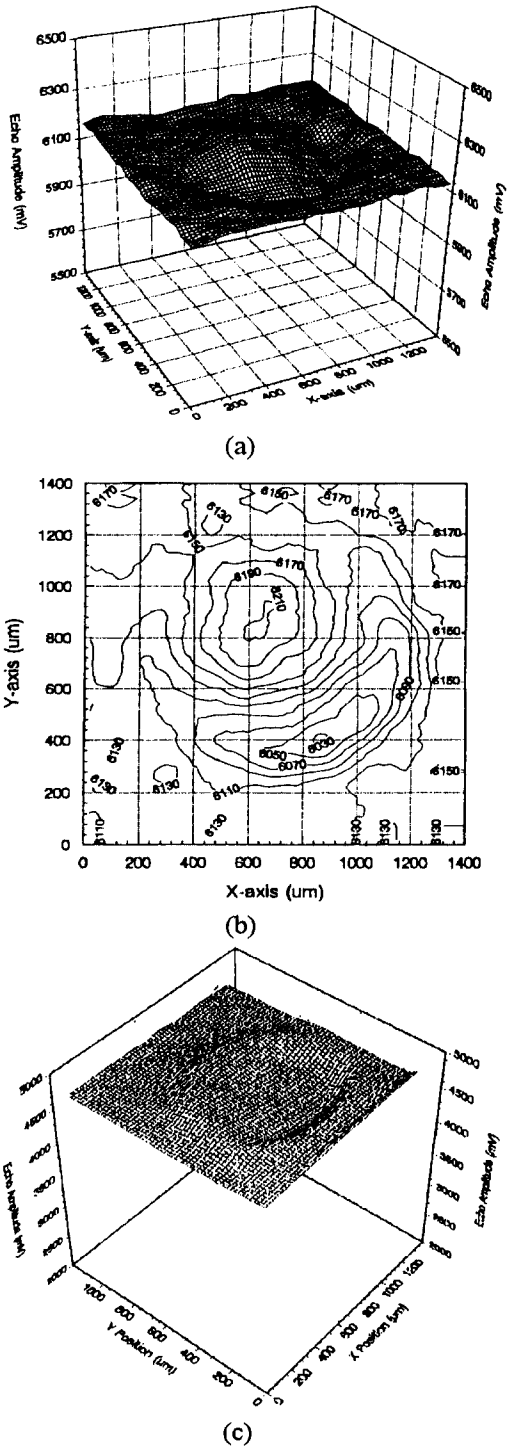

Fig. 8. (a) 3-D echo-amplitude map of the indent in glass-ceramic, (b) contour plot at surface focus, and (c) 3-D echo-amplitude map of the indent at 100 μm defocus.

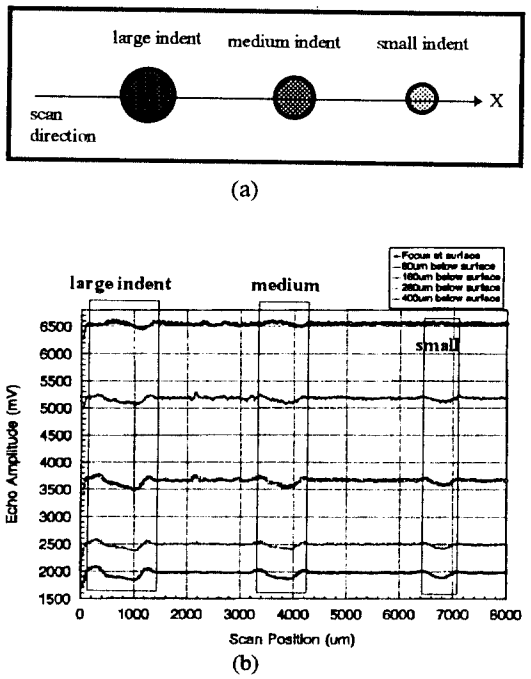

Fig. 9. (a) A schematic of three indents in glass-ceramic, and (b) line scans over the center of indents at various depths of focus.

the Hertzian indentation damage. The type of damage is classified as cone crack and subsurface microfractures In the former case, emminent damage, appearing as ring-shape cracks on the surface and thus relatively large cracks, is formed while in the latter case, produced is only indentation marks on the surface and distributed micro-sized cracks are hidden below the indent surface. Previous work done by authors showed that the normal-incident compressional ultrasonic waves were not sensitive enough to discern the normal cracks. However, considering that the near-surface part of the cone crack is normal to the surface, we demonstrated in this work that normal cracks can be detected if the cracks are relatively open comparing with the effective beam width of the ultrasonic waves. In this regard, we expect that the sensitivity of detecting normal cracks will be strongly influenced by the operating frequency of the transducer employed. The transducer used in this work has an operating frequency of 35 MH having the effective beam width of around 35 μm which is in fact much larger than the width of the opened normal cracks. By us-

ing a transducer with higher operating frequency that provides a waves having smaller beam width, measurement of normal cracks will be improved. Further evaluation is needed in this direction.

5. Conclusions

(1) The normal-incident ultrasonic compressional wave technique can be successfully applied to detect both cone cracks and subsurface micro-fractures produced by Hertzian indentation.

(2) The normal-incident ultrasonic compressional wave technique can detect normal cracks but it strongly depends on the width of their opening.

(3) Focusing of the transducer into the material (defocusing) provides information on the size of the subsurface micro-fracture damage of materials.

(4) The normal-incident ultrasound technique used in this work has demonstrated its accessibility to subsurface damage and, taking into account that machining processes generate subsurface damage, this technique may be applied to evaluate near-surface damage of materials after machining.

Acknowledgment

The authors are grateful to Dr. G. V. Blessing at NIST for helpful discussions on ultrasonic measurements and for making the ultrasonic measurement system available for this work. They are also grateful to Dr. Cai for the supply of mica-containing glass-ceramic specimen and associated micrographs. This work was sponsored in part by the U. S. Department of Energy, through the Cermaic Technology Project at the Oak Ridge National Laboratory, and by the Korea Institute of Science and Technology.

References

1. Ahn, H. S., Wei, L. and Jahanmir, S., "Non-Destructive Detection of Damage Produced by a Sharp Indenter in Ceramics," *Manufacturing Science and Engineering* Vol. 2 (PED-Vol. 68-2), pp. 955-964, ASME, 1994.
2. Ahn, H. S. and Achenbach, J. D., "Response of Line Focus Acoustic Microscope to Specimen Containing a Subsurface Crack," *Ultrasonics*, Vol. 29, pp. 482-489, 1991.
3. Cai, H., Kalceff, S. and Lawn, B. R., "Deformation and Fracture of Mica-Containing Glass-Ceramics in Hertzian Contacts," *J. Mater. Res*, Vol. 9, No. 3, pp. 762-770, 1994.
4. Chyung, C. K., in *Fracture Mechanics and Ceramics*, Bradt, R. C. et al. eds, Vol. 2, pp. 495-508, Plenum Press, New York, 1974.
5. Edwards, G. R., "Non-Destructive Testing of Engineering Ceramics," *British Ceram. Trans. J.*, Vol. 88, pp. 117-123, 1989.
6. Guiberteau, F., Padture, N. P. and Lawn, B. R., "Effect of Grain Size on Hertzian Contact in Alumina," *J. Am. Ceram. Soc.*, Vol. 77, No. 7, pp. 1825-1831, 1994.
7. Friedman W. D., Bhagat, A. R., Srinivasan, M, and Wilson, J., 1988, "An Assessment of Various Methods Which Detect Critical Surface Flaws in Sintered SIC," *Review of Progress of Quantitative Nondestructive Evaluation,* D. O. Thompson and D. E Chimenti, Eds, Vol. 5B, pp. 1509-1518.
8. Jahanmir, S., Machining of Advanced Materials, *Proceedings of the Int. Conf. on Machining of Advanced Materials*, Gaithersburg, MD,July 20-22, 1993, NIST Special Publication 847, National Institute of Standards and Technology, 1993.
9. Lawn, B. R., *Fracture of Brittle Solids,* Cambridge Univ. Press, U. K., 1968.
10. Lawn. B. R. and Marshall, D. B., "Indentation Fracture and Strength Degradation in Ceramics," pp. 205-209 in *Fracture Mechanics of Ceramices*, Vol. 3, R. C. Bradt et al. eds., Plenum, New York, 1978.
11. Lawn, B. R. and Swain, M. V., "Microfracture Beneath Point Indentations in Brittle Solids," *J. Material Sci.*, Vol. 10, pp. 113-122, 1975.
12. Lawrence, C. W., Scruby, C. B., Briggs, G. A. D. and Dunhill, A., "Crack Detection in Silicon Nitride by Acoustic Microscopy," *NDT Int.*, Vol. 23, pp. 3-8, 1990.
13. Mulhearn, T. O., "The Deformation of Metals by Vickers-Type Pyramidal Indenters," *J. Phys. Solids*, Vol. 7, pp. 85-96, 1959.
14. Rocenswaig, A., Opsal, J., Smith, W. L., and Willenburg, D. L., 1985, *Appl. Phys. Lett.*, Vol. 46, pp. 1013-1015.
15. Xu, H. H. K., Wei, L., Padture, N. P. and Lawn, B. R., "Effect of Microstructural Coarsening on Hertzian Contact Damage in Silicon Nitride," *J. Materials Science*, (in press) 1995.

16. Yamanaka, K. and Enomoto, Y., "Observation of Surface Cracks with Scanning Acoustic Microscope," *J. Appl. Phys.*, Vol. 53, pp. 846-850, 1982.

17. Yamanaka, K., Enomoto, Y. and Tsuta Y., "Acoustic Microscopy of Ceramic Surface," *IEEE Trans. Sonics and Ultrasonics*, Vol. SU-32, pp. 313-319, 1985.